BioOne COMPLETE

Formation, Migration, and Morphodynamic Alteration of 50 Channel Bars in Darjeeling Himalayan Piedmont Zone, India

Authors: Dhali, Md Kutubuddin, and Mukhopadhyay, Sutapa

Source: Air, Soil and Water Research, 13(1)

Published By: SAGE Publishing

URL: https://doi.org/10.1177/11786221209414436

BioOne Complete (complete.BioOne.org) is a full-text database of 200 subscribed and open-access titles in the biological, ecological, and environmental sciences published by nonprofit societies, associations, museums, institutions, and presses.

Your use of this PDF, the BioOne Complete website, and all posted and associated content indicates your acceptance of BioOne's Terms of Use, available at www.bioone.org/terms-of-use.

Usage of BioOne Complete content is strictly limited to personal, educational, and non - commercial use. Commercial inquiries or rights and permissions requests should be directed to the individual publisher as copyright holder.

BioOne sees sustainable scholarly publishing as an inherently collaborative enterprise connecting authors, nonprofit publishers, academic institutions, research libraries, and research funders in the common goal of maximizing access to critical research.

Downloaded From: https://complete.bioone.org/journals/Air,-Soil-and-Water-Research on 28 Mar 2024
Terms of Use: https://complete.bioone.org/terms-of-use

Formation, Migration, and Morphodynamic Alteration of 50 Channel Bars in Darjeeling Himalayan Piedmont Zone, India

Air, Soil and Water Research
Volume 13: 1–17
© The Author(s) 2020
Article reuse guidelines:
sagepub.com/journals-permissions
DOI: 10.1177/1178622120941436
SAGE

Md Kutubuddin Dhali and Sutapa Mukhopadhyay
Department of Geography, Visva-Bharati, Santiniketan, India.

ABSTRACT: Channel bars are common, striking fluvio-geomorphic depositional features of alluvial rivers. The study of this article has aimed to investigate the formation, migration, and morphodynamic alteration of channel bars (n = 50) in gravel braided alluvial rivers in Darjeeling Himalayan Piedmont zone. Dynamics of micro to meso bar deposition is mainly accomplished by the channel gradient, huge upstream landslide, and variation of discharge. Multi-criteria analysis method has been used to explain the variation of principal component analysis (PCA1, PCA2, and PCA3), both monsoon to post-monsoon. Bridge scouring, empirical aggradation, and degradation values are 0.1 to 1.05 m and 200 kgm^2s^{-3}-2500 kgm^2s^{-3}-2500 kgm^2s^{-3}. Migration, re-generation, and degradation of the micro bars with their optimum morphology show changes during the rainy season. In the upper (Δu_A), middle (Δm_A), and lower ($\Delta 1_A$) piedmont region, the bar dynamic area are 0.12 to 0.71, 0.12 to 2.83, and 0.10 to 5.43 km^2, respectively. In total, 58% to 72% stability of the channel bars is observed in the upper piedmont region. The coefficient of determination (R^2) of channel bar area and width shows positive (0.63) relation.

KEYWORDS: Darjeeling Himalayan piedmont zone, channel bar formation, MCA methods, union and intersection, bridge scouring, morphodynamic alteration

RECEIVED: June 2, 2020. **ACCEPTED:** June 16, 2020.

TYPE: Original Research

FUNDING: The author(s) received no financial support for the research, authorship, and/or publication of this article.

DECLARATION OF CONFLICTING INTERESTS: The author(s) declared no potential conflicts of interest with respect to the research, authorship, and/or publication of this article.

CORRESPONDING AUTHOR: Md Kutubuddin Dhali, Department of Geography, Visva-Bharati, Santiniketan, West Bengal, 731235, India. Email: kutubgeo@gmail.com

Introduction

Running water landform processes govern the hydro-morphological amplitude[1-6] and examine the calibre of water-sediment interaction towards the development of channel bar sequences as a micro-riverine unit of foothill riverbed. Such kind of unit has an ample scope for studying its formation, migration in terms of dynamism, and stability which defer with scale, dimension, sediment setting, channel gradient, variation of discharge, flow bifurcation, channel pattern, and seasonal incoming sediment, and so on.[7-10] Over the past several decades, sediment transportation and regular deposition of many alluvial large rivers in the world in lower regions especially coastal areas has continuously shown a decrease.[11-16] The Mississippi River (Mississippi to Gulf of Mexico, 400 MT before 1900 to 172 MT during last 3 decades) and Yangtze River (Yangtze to East China Sea, 40% decrease in 2000s) are examples for decreasing annual suspended sediment.[17-20] So, the scenario of aggradation and degradation is rapidly changing.

Formation of channel bar by the processes of sediment transportation is a natural process and their morphological changes are more remarkable depending upon the channels hydrological components.[21] North Bengal rivers of Himalayan foothill region gain their 'health' in monsoon time and carry large amount of coarse sediment especially Teesta, Torsa, and Jaldhaka.[22-24] New deposition and destruction of channel bars are much more active during July-August months of Indian subcontinent due to the interaction of varied geo-hydrological processes. But many of large, medium, and small rivers are affected by construction of dam, barrage, and bridge[17,25-28] which strongly influence channel discharge, velocity, and rate of sediment transportation. In the monsoon phase, maximum flash flood zone spreads in the lower section of the bridge and as a consequence effect channel bars are formed with the flood prone large boulders. Moreover, the variations in gradient, sediment characteristics, velocity, discharge amount formulate the number, shape, and dynamicity of the channel bars of this foothill region. The increased rate of incoming sediments also brings change in the morphological characteristics and is responsible for channel bar migration.[4,29-31]

Among all of the previous studies, for the present research analysis, some notable works such as sediment setting of channel bars in lower Mississippi River,[19,20] formation of mouth bars in Yellow River,[4] generation of gravel bars in Loire River,[32] mechanism of river mouth bar in Mossy Delta,[33] mechanism of gravel bar in Mekong River,[34] development of braided bar in Brahmaputra-Jamuna River,[35-37] bar formation due to scouring process,[38] flow mechanism and numerical modelling of channel bars,[8,39-43] evolution of large bars in Jamuna River,[44] point bar deposition in Peace River,[45] and significance of mid-channel bar in Dane River are considered.[46] This study has focused on the dynamic nature of channel bars in Darjeeling Himalayan piedmont zone. The study has also included migration rate of 50 channel bars since 2000s on the basis of different intensive field visits and with the aid of different empirical equations with geo-statistics techniques. This is a novel research which has monitored the stability and instability of channel bars and is very vital for planners, environmentalists, agriculture and forest department, authority of environmental management, and different river institutions.

Creative Commons Non Commercial CC BY-NC: This article is distributed under the terms of the Creative Commons Attribution-NonCommercial 4.0 License (https://creativecommons.org/licenses/by-nc/4.0/) which permits non-commercial use, reproduction and distribution of the work without further permission provided the original work is attributed as specified on the SAGE and Open Access pages (https://us.sagepub.com/en-us/nam/open-access-at-sage).
Downloaded From: https://complete.bioone.org/journals/Air,-Soil-and-Water-Research on 28 Mar 2024
Terms of Use: https://complete.bioone.org/terms-of-use

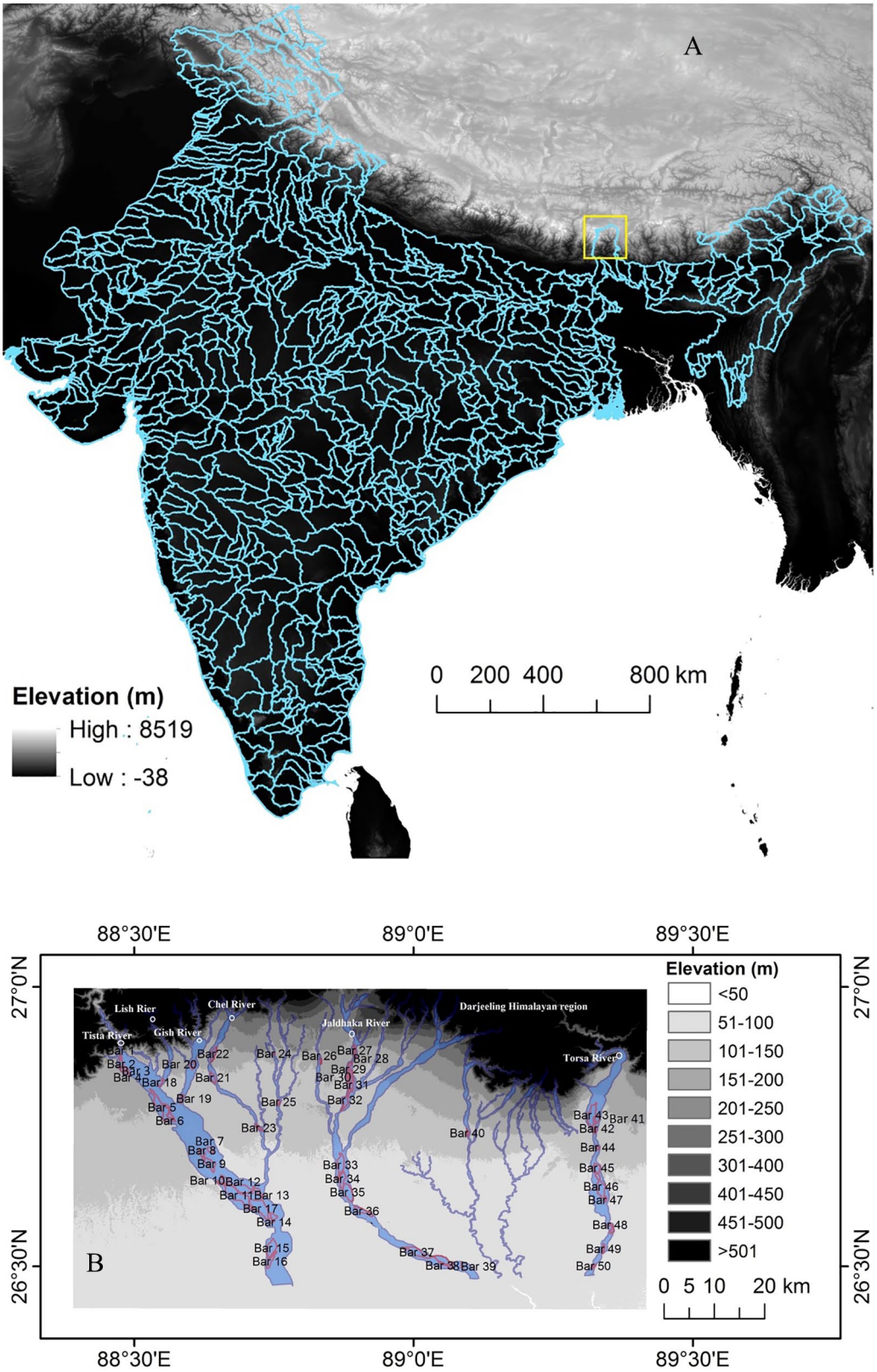


Figure 1. (A) Major basin and sub-basins in Indian subcontinent with change of elevation; yellow box indicates area of this study. (B) River system and subsystem of Darjeeling Himalayan foothill zone; Teesta, Lish, Gish, Chel, Mal, Murti, Kurti, Naora, Jaldhaka, Daina, Torsa are selected for sample size.

Study Sites, Geology, and Tectonic Setup

This study has been done in the piedmont section of the Eastern Himalayas drained Lish, Gish, Chel, Mal, Neora, Murti, Juranti and Jaldhaka, Teesta, and Torsa rivers (Figure 1). All these rivers are a part of the Ganga-Brahmaputra subsystem and are much younger in age as they are present in the piedmont zone of the Himalayas.[47,48] All these rivers originate at a very high elevation of above 1500 to 2000 m and end

Downloaded From: https://complete.bioone.org/journals/Air,-Soil-and-Water-Research on 28 Mar 2024
Terms of Use: https://complete.bioone.org/terms-of-use

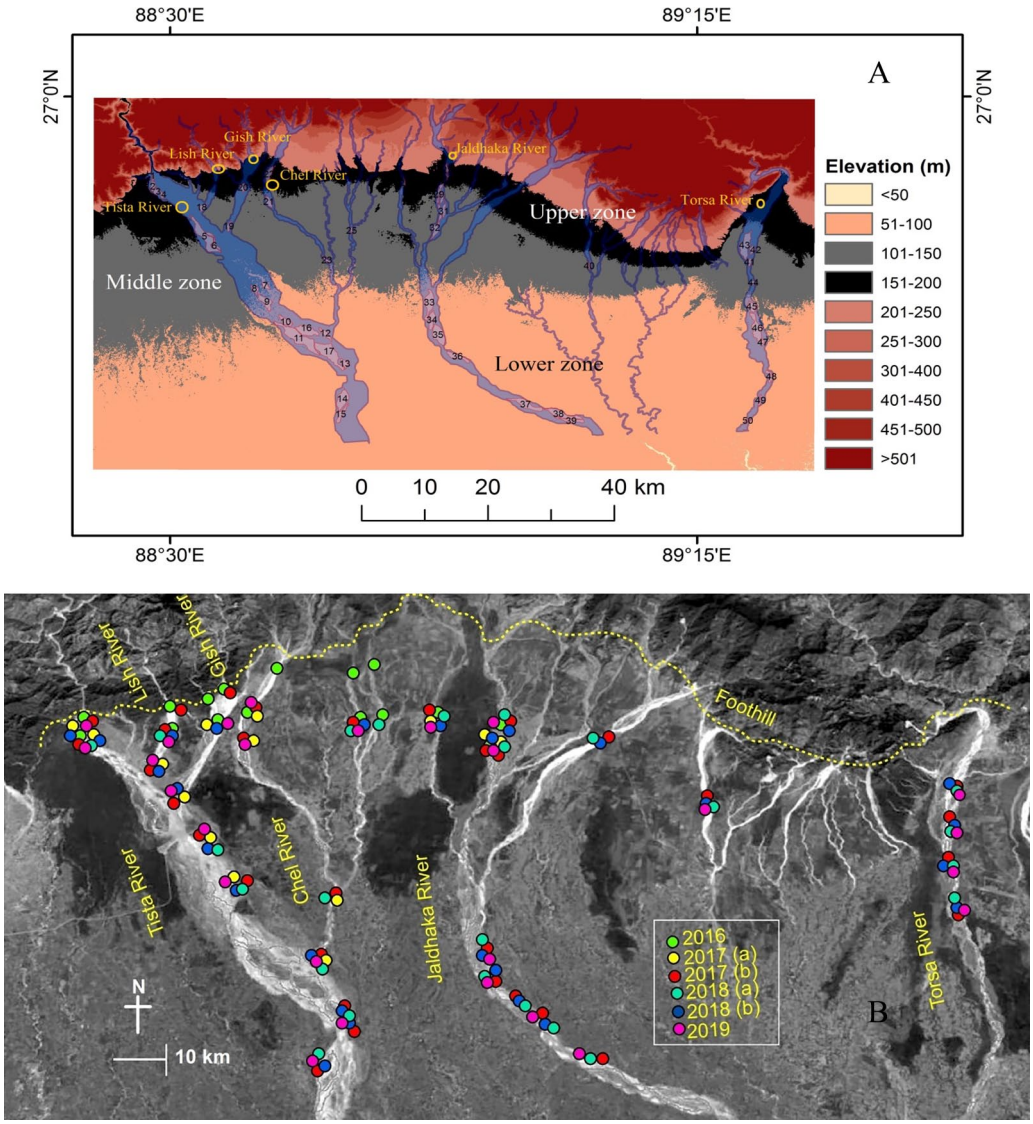


Figure 2. (A) Major 3 zones for analysis of morphodynamic alteration of channel bars in Darjeeling Himalayan foothill zone; Upper zone (>150 m), Middle zone (100-150 m), and Lower zone (<100 m). (B) Different field surveys are conducted during the work since 2016 on the basis of above zonation.

jointly at around 50 to 300 m elevation. Considering the geomorphological and hydrological disparity, the piedmont area of Darjeeling Himalayas has been classified into 3 specific zones: Upper (>150 m), Middle (150-100 m), and Lower (<100 m) (Figure 2; Table 1). The rivers, which are considered in this study, have the major orientation from NE to SW, all with prominent seasonal variation. These tributaries are mainly non-perennial excepting large rivers such as Teesta, Torsa, and Jaldhaka. These non-perennial streams form small alluvial fans at their debouching points and contain numerous minor faults along their courses which are active in nature.[49-52] As these rivers are mainly dependent on seasonal rainfall, the distribution of the boulders is also controlled by the rainfall intensity and pattern. The region is mainly covered by the young quaternary sediments which are the most recent deposition. However, exposures of Gondwana group of rocks are noticed along the sections of Gish Nadi and Ramthi Nala. Prominent quartzite bands are visible in several rocks of this region. The tectonic setup of the region indicates that the region is tectonically very active. Being a part of the Himalayan Foreland Basin, it contains the most active fault, that is, the Main Frontal Thrust.[48] This fault line passes through the course of these rivers which is one of the reasons for the development of several minor faults in the course of these rivers,[49-51] and at many places, the channels take straight and right-angle bends. The foreland basin is characterised by axial and traverse drainage patterns.[53] The deposition from the rivers of the foreland basin controls the dynamics of the basin since the Pleistocene. The presence of numerous fluvial mega fans[53] and many small mountains attached micro fans is the main characteristics of the Eastern Himalayan mountain front. Gish River to the Neora River is an indicator of the neo-tectonic activities that had taken place here. Two groups of faults are noticed here, namely, the east-west trending faults along the mountain fronts and the NNE-SSW to NNW-SSE trending faults along with the river courses such as Gish, Lish, Chel, and Lethi rivers.

Downloaded From: https://complete.bioone.org/journals/Air,-Soil-and-Water-Research on 28 Mar 2024
Terms of Use: https://complete.bioone.org/terms-of-use

Table 1. Location and geomorphic characteristics of the sample sites of channel bar of some major rivers such as Teesta, Torsa, Jaldhaka, and their prime tributaries in Darjeeling Himalayan foothill zone.

ZONE	NAME OF THE RIVER	IDENTIFIED SITES	NUMBERING OF THE BARS	AVERAGE HEIGHT	SLOPE	NO. OF BARS	HYDRO-MORPHOLOGICAL CHARACTER OF THE CHANNEL
Upper	Teesta, Leesh, Gish, Chel, Murti, Kurti, Jaldhaka, Torsa	Sevoke, Bagrakote, Odlabari, Manabari, Damdim, Nagrakata, Birpara, Hasimara	Bars 1-3, 20, 22, 24, 26-29	>150 m	8°-25°	10	Large-, medium-, and lower-sized channel bar, gravel and pebble dominant, variation of gradient, river discharge and stream power, low channel bar dynamicity
Middle	Teesta, Gish, Chel, Jaldhaka, Rehti, Torsa	Lataguri, Moulani, Bhandani, Magurmari, Jaldapara	Bars 4-9, 18-19, 21, 23, 25, 30-32, 40-44	100-150 m	5°-15°	19	Micro to mega channel bars, gravel-sand dominant sediments, huge aggradation, at the downstream of the bridge dominant seasonal variation in channel bar morphology, riverbed aggradation
Lower	Teesta,, Jaldhaka, Torsa	Domohani, Maynaguri, Dhupguri, Mathurabagan, Patlakhawa	Bars 10-17, 33-39, 45-50	<100 m	<10°	21	Large to medium channel bars, coarse to medium sand deposition, channel bar transformation rate high, intensive braided pattern

Data and Methods

The whole study was developed in 3 individual stages: primary data, secondary data, and geospatial technique. Primary data survey was conducted for the past 4 years (2015-2019) especially during the beginning of the winter season, end of the winter season, and monsoon season. Secondary data were collected from the Survey of India (Kolkata) for Topographical map and Landsat images were downloaded (Landsat 8) from USGS Earth Explorer.

MCA models

For understanding the dynamic nature of the formation of the bar in piedmont region, multi-criteria analysis has been applied,[54-56] Principal component analysis method (PCA) is used for proper clarification. Geo-hydrological components such as bed slope, water discharge, gradient, bed elevation, velocity, roughness, specific stream power, and shear stress have considered as parameters for this analysis. Some of the geo-hydraulic equations are supported for the explanation of PCA consistencies. Those are 'Cross-sectional area (A) = W × D', Water Discharge (Q) = A × V, Wetted Perimeter (WP) = W + D, Hydraulic Radius (HR) = A/WP, Mean Shear Stress $\tau_0 = \rho g h S$, Stream Power, $\Omega = \rho g Q S$, Specific Stream Power$(\omega) = \Omega / W$, Velocity$(v) = (R^{0.67} s^{0.5}) / n$. Where '$W$' is mean width and '$D$' is mean depth, '$A$' is cross-sectional area and 'V' is mean velocity, 'WP' is wetted perimeter, 'τ_0' is shear stress, 'ρ' is the water density $(1000\,\mathrm{kg/m^3})$, 'g' is the acceleration due to gravity $(9.8\,\mathrm{m/m^2})$, 'h' is flow depth and 's' is the channel slope (here slope indicates gradient, $\tan^{-1}$ gradient value is slope), 'Ω' is stream power, ω is specific stream power, 'n' is Manning equation, 'R' is hydraulic radius.[57] PCA1, PCA2, and PCA3 are the respective levels of consistency measurement of selective components. The consistency measurement is done with the help of IMBS SPSS 22 software.

Rate of erosion and bar aggradations

Rate of erosion in upstream and downstream of the bridge indicates the major zone of agglomeration. For this purpose, one hydrodynamic mathematical equation is employed for the outcome of the results for bed erosion with suspended load relation.[58]

$$\frac{dz}{dt} = \frac{1}{2}\frac{Csed}{\gamma}\left(\frac{vg - vo}{sa}\right)^2 \quad (1)$$

where 'dz' erosion rate, 'dt' is time, so 'dz/dt' is the rate of bed erosion due to time duration; '$Csed$' is river bedload sediment; 'vg' is water velocity of the first point (selective first segment point of the river); 'vo' is water velocity at the endpoint (selective end segment point of the river); '$vg - vo$' is water velocity difference between first point and end point; and sa is rock susceptibility.

Analysis of bridge scouring address in different points

Richardson's scouring equation[59] is applied for the analysis of the rate of erosion in different bridge points at the beginning of winter and end of the winter season since 2015. This equation is directly related to bridge scouring condition of this place which is a better observation of aggradations and degradation. The equation is as follows:

$$\frac{y_s}{y_1} = 2 \cdot k_1 \cdot k_2 \left(\frac{a}{y_1}\right)^{0.65} Fr1^{0.43} \quad (2)$$

where y_s is scour depth (m), y_1 is flow depth just upstream of the pier (m), k_1 is a correction for pier shape, k_2 is a correction for flow angle of attack of flow, a is Pier width (m), $Fr1$ is Froude number.

Downloaded From: https://complete.bioone.org/journals/Air,-Soil-and-Water-Research on 28 Mar 2024
Terms of Use: https://complete.bioone.org/terms-of-use

Interpolation and union methods

We have classified the dynamicity of bar size, width, and length into 5 general categories by the following traditional statistical class boundary methods (C = 1 + 3.322logN, 6.44). On the basis of variation of dynamicity, real figure of data and the field verification, 5 classes have been chosen for better explanation. Classes of channel bar with longest width dynamicity are <0.25, 0.25 to 0.50, 0.50 to 0.75, 0.75 to 1.00, and >1.00 km. The dynamicity of channel bar size classes are <0.25, 0.25 to 0.50, 0.50 to 0.75, 0.75 to 1.00, and >1.00 km^2. The method of interpolation and union has helped to analyse the stability of the mid-channel bars in respective sites. With the help of interpolation method, it was possible to identify the effective bar development areas which also include the areas where the maximum deposition of bars has taken place. The method of union could depict the common areas from the interpolation data where there is constant bar formation since the 2000s. These are very effective methods which are very helpful to understand the changing zones of bar formation, development of new zones, stable zones with continuous deposition, and also the zones which show degradation. These methods were applied with the help of ArcGIS 10.2.2 for getting the result of the net stable area and also the whole bar genesis region.

Geospatial techniques

Some of the importantly supported mappings are done by geospatial techniques in different software such as ArcGIS 10.2.2, Global Mapper 18, and Surfer 11. A basic morphometric technique like the change of surface elevation and slope aspect is developed by IDW method and Raster Interpolation methodology in ArcGIS 10.2.2. Total Station [FOIF (EL302A)], hand GPS (Garmin eTrex, VISTA HCX, horizontal ground accuracy ± 3 m), and clinometers are used in the winter season where bar surface is dry and open also. Cross-profile of different bars is prepared by Global Mapper 18 with the help of riverbed DEM (Digital Elevation Model) of Total Station [FOIF (EL302A)] and hand GPS (Garmin eTrex, VISTA HCX, horizontal ground accuracy ± 3 m) data. Riverbed and bars DEM are also made by Surfer 11 with the help of TS data.

Results

Hydro-geomorphic integrity

Hydro-geomorphic component variation of Darjeeling Himalayan piedmont rivers is very dynamic in pre-monsoon to post-monsoon.[12] After the rainfall, mountain rivers are very energetic in the Eastern Himalayan region. In the rainy season, the amount of rainfall is 100 mm approximately per day in this region.[60] The mean discharge of Teesta, Lish, and Gish is 3000 to 5000 m^3s^{-1}, 0.25 to 254.7 m^3s^{-1}, and 0.08 to 630.2 m^3s^{-1}.[61] Peak discharge becomes maximum after a few fresh rain spell in monsoon. Bar formation of the upper, middle, and lower zones of the piedmont area also depends on this hydro-geomorphic variation. Integrity is an interdisciplinary part of any kind of relationship of natural science. The variations of hydro-morphological components have the major role for the evolution of channel bars in North Bengal fluvial system and subsystem. The interrelation between those is very strong and its integrity depends on spatial-temporal scale. Bed elevation, water velocity, mean width, mean depth, wetted perimeter, hydraulic radius, cross-sectional area, water discharge, stream power, bed slope, inertial force, bed elevation (Manning roughness), water depth (active), shear stress, and specific stream power were indicators of hydro-geomorphic integrity. In the rivers of Teesta, Lish, Gish, Chel, Mal, Naora, Murti, and Kurti, PCA1 provided 86.67% hydro-geomorphic diversity, PCA2 provided 53.33%, and finally PCA3 indicated 66.67% diversity (primary data survey, 2015-2017). The same scenario is also observed in eastern side of the rivers such as Jaldhaka, Daina, and Torsa; PCA1 shows 93.33%, PCA2 is 53.33% and PCA3 is 53.33% hydro-geomorphic diversity (2017-2019) (Figure 3). But individual consistency of strangeness of different components has shown quite change from PCA1 to PCA2, PCA2 to PCA3. Channel bar formation, migration, and change of geomorphic characters are also regulated by these dynamic hydro-geomorphic characters.

Riverbed erosion and aggradation process

Alluvial rivers in the Himalayan foothill region are very dynamic,[47,48,62] especially in terms of deposition.[10] The mobile deposition is a common feature of the riverbed in Darjeeling Himalayan foothill zone. Many times, seasonal deposition of the past is eroded by the huge amount of water mass and seasonal flood. River curvature such as meandering, sinuosity, and anabranching have high influence on the temporal deposition of the channel. A better explanation of aggradation and degradation in different points of the riverbed is explained by bed erosion with suspended load relation which is widely developed by Foley[58] and Dhali and Sahana.[21] The value of this hydrodynamic empirical equation since 2015, in the dry season of Teesta near Sevoke, Lish near Bagrakote, Gish near Uttar Fulbari, Chel near Odlabari, Mal near Mal bazaar, Neora near Neora bridge, Kurti near Chalsa, Jaldhaka near Nagrakata, Torsa near Hasimara varies from 200 to 2500 $kg\,m^2s^{-3}$. The maximum degradation is noticed in selected points of Jaldhaka which has a high empirical value such as 1978.952, 2182.18, and 2542.963 $kg\,m^2s^{-3}$ in respective dry period (Table 2). A lower value shows the high rate of riverbed aggradations. These values have depicted that upper and lower parts of the bridges are less erosive, and the erosive nature is quite high nearby to the bridges.

Bridge scouring and channel bar deposition

In this study, it has been witnessed that the scouring processes have significant extent and the result of Richardson's scouring equation has prominently delineated the changes of velocity

Downloaded From: https://complete.bioone.org/journals/Air,-Soil-and-Water-Research on 28 Mar 2024
Terms of Use: https://complete.bioone.org/terms-of-use

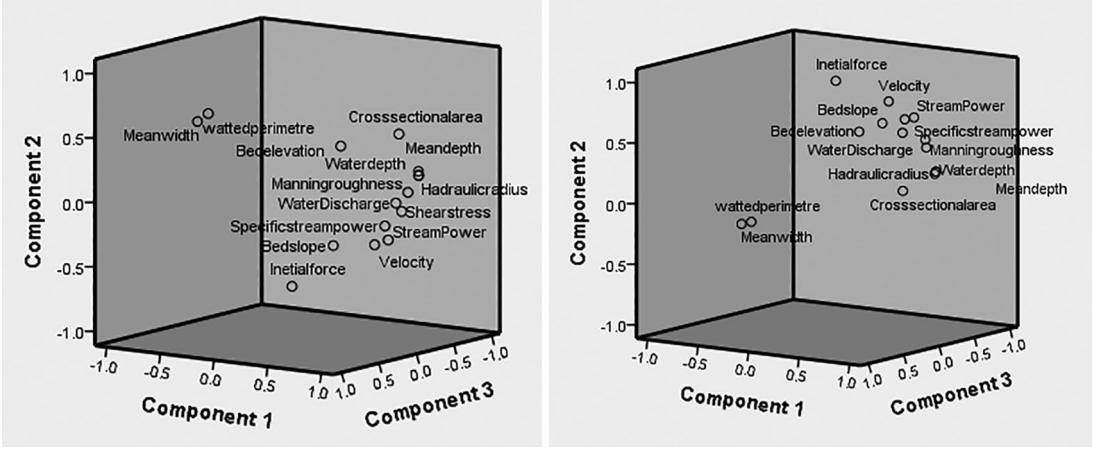


Figure 3. MCA (multi criteria analysis) of different components on hydro-geomorphological integration in channel bar dynamicity, in the left figure indicated MCA of Teesta, Lish, Gish, Chel, Mal, Naora, Murti and Kurti (2016-2018) right figure indicated MCA of Jaldhaka, Daina and Torsa (2017-2019).

with depth in accordance with the process. The depth of bridge scouring of Teesta, Torsa, and Jaldhaka are 1.05, 0.55, and 0.64 m at Sevoke, Hasimara, and Nagrakata. Others tributaries such as Lish, Gish, Mal, Murti, Kurti, Neora, Chel, Dhorla show 0.10 to 0.40 m scouring depth (Figure 4). The values of scouring along the studied channel also depict the alternative change of sediment regime which is strongly interrelated with the stream energy and velocity distribution. The observed mean D50 value shows an alteration regime of bedload distribution near the bridge.[10] The empirical equation values in Teesta, Torsa, and Jaldhaka provided 8.2585, 9.6272, and 7.1317 which depicts the high degradation behaviour. The empirical values of River Chel near road and railway bridge show 5.388 and 4.3017 where real scouring depth are 0.82 and 1.06 m (2015-2019). The hydrological parameter and sediment mean D50 values, both are responsible for the changing nature of the regime which has become a cause of huge deposition just after the bridge and sudden release of energy, aggravate the depositional rate with the resulted landform. Some of riverbed cross sections have also provided a change of bar surface and active channel depth. In the upper part of the bridge in Jaldhaka River; AB, CD, and EF are riverbed cross sections. AB provided 174 to 178 m surface elevation, CD is 169 to 166 m, and EF is 168 to 162 m. The elevation drop moves an active channel from those places. PQ_, RS, and XY are other riverbed cross sections in the lower part of the bridge. PQ highest and lowest surface elevation is 155 to 145 m, RS is 155 to 145 m, and XY is 150 to 135 m (Figure 5). River bars are affected by some of the anthropogenic activities such as bridge construction and seasonally boulder, pebble, and cobble lifting of the riverbed. Lifting of the large size sediment on the riverbed has also decreased the bar elevation, and in some points, bar mean angle with the related mean direction of the active channel has also migrated.

Configuration of bar morphological attributes

From the upper, middle, and lower zones of piedmont areas, 10, 19, and 21 channel bars have been selected, respectively, for the study. Different types of channel bars have observed in this foothill region (Figure 6). These 50 mid-channel bars are of large, medium, and small size. For configuration of bar morphological attributes, 18% (>3 km^2), 44% (>1.5 km^2), and 38% (<1.5 km^2) are of large, medium, and small size. All these bars covered 20% (n = 10), 38% (n = 19), and 42% (n = 21) of the total bars of the respective zones. The orientation of the bars direction changes from north to south, south to west, and south to east in response to the river flow direction. The relative height of the bar varies from 5.1 to 0.2 m, 5.1 to 0.1 m, and 2.2 to 0.6 m respectively in the different altitudinal zones. The nearest bar active channel water depth of dry season covered 2.6 to 0.1 m, 1.8 to 0.1 m, and 2.6 to 1.1 m.

Reach-wise variation in longest length of channel bars

Mean active channel flow is continuously dynamic[63] because the braided nature and channel bars have shifted from their original position in the past 20 years. From the field observation, unstable bars are affected by active flow orientation of the sites. Multiple channel pattern and change of sediment deposition in mid- to side-channel are quite changed by the nature of flow.[47] Mean bar directions are south-south east (SSE) to south-south west (SSW) from true north and mean flow direction is south-south east (SSE). Mid-channel bars and related active channel flow are quite shifted towards leftbank from the source of the river. The important fact is that the coefficient of determination between the shifting of bars and active channels has a very strong positive relation (R^2 = .9837). So the result indicates that mean bar angles are affected by the mean active flows. After the complete study, from the geometry analysis methods of ArcGIS 10.2.2, it is revealed that in the upper part of the piedmont zone, the dynamic behaviour of channel bars' longest width is very low (<0.25 km) to moderate (0.50-0.75 km). In the upper zone, serial number of channel bar 1 and bars 24 to 28 show <0.25 km dynamic nature, bars 2 and 3 show values 0.25 to 0.50 km, and similarly bars 20, 22, and 29

Downloaded From: https://complete.bioone.org/journals/Air,-Soil-and-Water-Research on 28 Mar 2024
Terms of Use: https://complete.bioone.org/terms-of-use

Table 2. Empirical calculation value of suspended sediment and erosion for analysis of aggradation in dry period of some selected part of the given rivers in Darjeeling Himalayan Piedmont zone, India.

RIVERS	PLACES	X	Y	DURATION	$\Delta_{t(i)}$ kgm^2s^{-3}	$\Delta_{t(ii)}$ kgm^2s^{-3}	$\Delta_{t(iii)}$ kgm^2s^{-3}	ΣT kgm^2s^{-3}	Δ_t kgm^2s^{-3}	OBSERVATION BASED ON SITE LOCATION
Teesta	Near Sevoke, downstream Sevoke bridge	26°51′55.72″ N-26°52′46.61″N	88°28′37.48″ E-88°28′50.01″E	4 y	902.9227	1500.163	846.0331	3249.119	1083.04	High scouring, upstream sediment, huge degradation
Lish	Bagrakote, near Lish bridge	26°52′3.93″ N-26°52′7.52″N	88°33′57.26″ E-88°33′53.84″E	5 y	253.7992	324.6994	275.7253	854.2239	284.7413	Bed elevation increase
Gish	Uttar Fulbari, near Gish bridge	26°52′33.62″ N-26°52′45.14″N	88°36′58.90″ E-88°36′36.09″E	5 y	255.0956	219.6062	216.0071	690.7089	230.2363	Bed elevation increase
Mal	Mal bazaar, near Mal bridge	26°52′56.40″ N-26°53′1.53″N	88°45′2.80″ E-88°45′2.15″E	5 y	418.8475	205.0643	558.2877	1182.199	394.0665	Lower degradation
Neora	Neora bridge, up and downstream	26°52′50.35″ N-26°53′4.68″N	88°46′21.42″ E-88°46′20.12″E	5 y	338.3692	301.5965	207.2432	847.2089	282.403	Lower degradation
Kurti	Chalsa, up and downstream of Kurti bridge	26°52′51.78″ N-26°52′56.13″N	88°47′31.90″ E-88°47′33.19″E	5 y	389.0415	1000.371	318.8639	1708.276	569.4255	Moderate degradation
Murti	Chalsa, up and downstream of Murti bridge	26°52′23.39″ N-26°52′53.40″N	88°49′45.46″ E-88°49′56.37″E	5 y	251.0522	314.7046	166.0999	731.8566	243.9522	Lower degradation
Jaldhaka	Nagrakata, up and downstream of bridge	26°52′16.12″ N-26°53′2.58″N	88°53′48.19″ E-88°53′39.76″E	5 y	1978.952	2182.18	2542.963	6704.094	2234.698	High degradation, huge lower part aggradation
Torsa	Hasimara, up and downstream of bridge	26°43′57.40″ N-26°44′52.15″N	89°19′21.11″ E-89°19′25.55″E	3 y	697.5215	732.8335	1877.484	3307.839	1102.613	Huge lower part aggradation after bridge

Downloaded From: https://complete.bioone.org/journals/Air,-Soil-and-Water-Research on 28 Mar 2024
Terms of Use: https://complete.bioone.org/terms-of-use

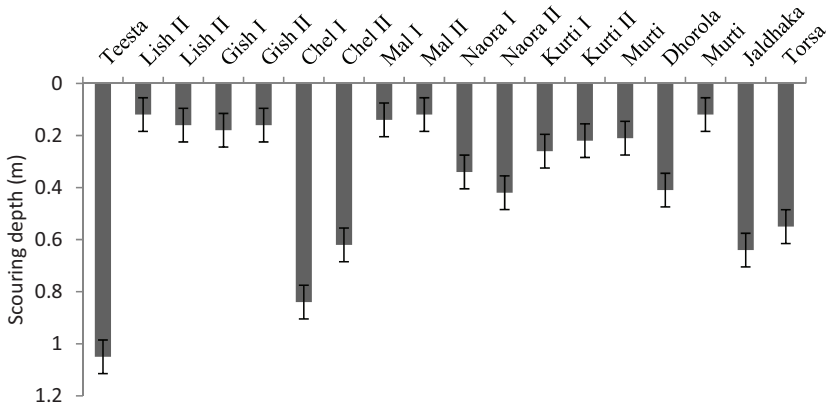


Figure 4. Scouring depth of different bridges (I – railway and II – road) in the month of post-monsoon phase, Darjeeling Himalayan piedmont region.

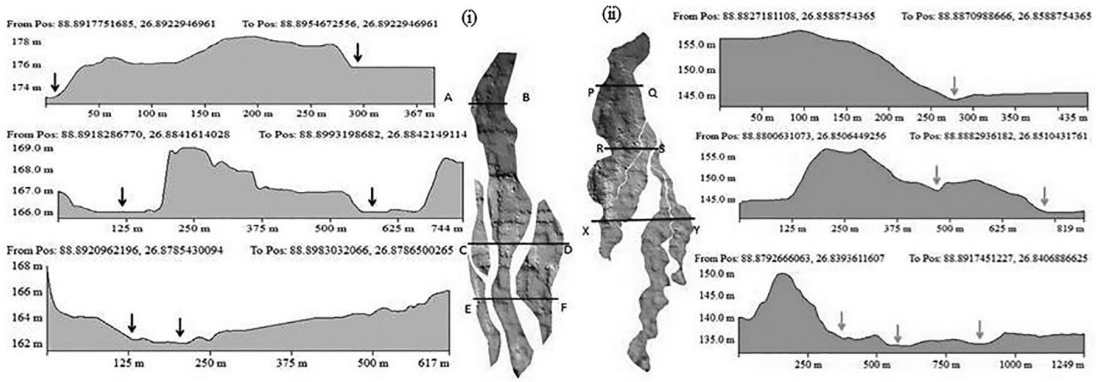


Figure 5. (i) Configaration of channel bar in Nagrakata bridge upper part, Jaldhaka River. AB, CD, and EF are respective elevation profiles which indicate bar surface morphology in different sections. (ii) Channel bar morphology in lower part of the bridge. PQ, RS, and XY are the major cross sections of bar surface elevation. Blue arrow indicates the present active channels.

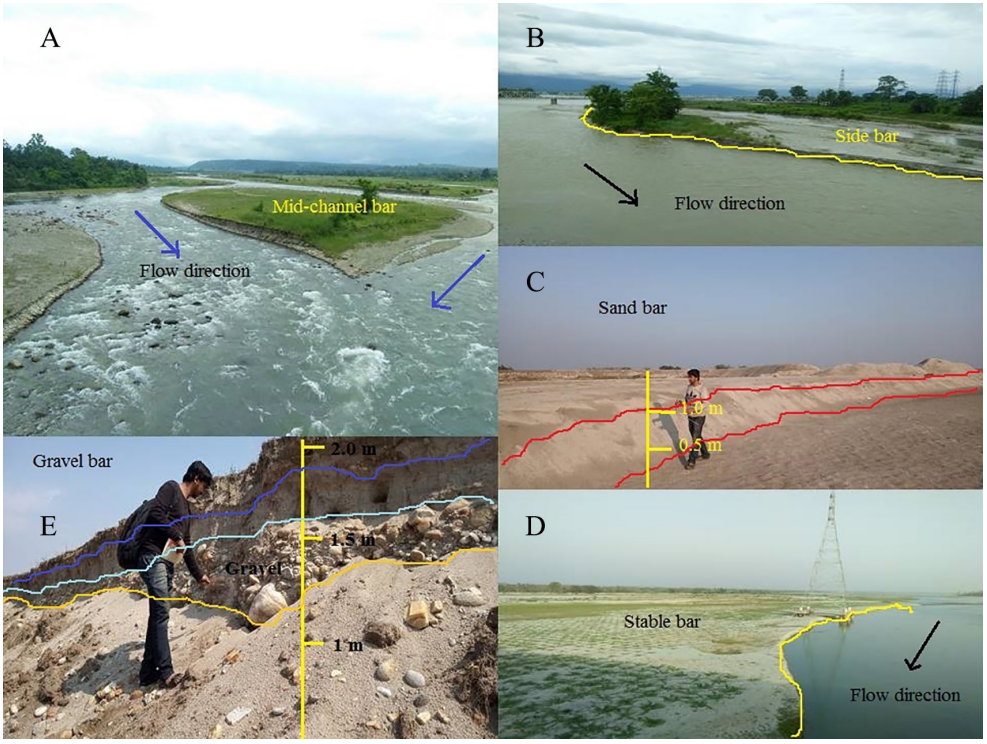


Figure 6. Various types of channel bars in Darjeeling Himalaya foothill zone: (A) mid-channel bar in Jaldhaka River near Nagrakata bridge, (B) side channel bar in Torsa River near Hasimara road bridge, (C) sand bar in Teesta River near Maynaguri, (D) stable channel bar in the lower part of Torsa River, and (E) Gravel channel bar in Teesta River near Sevoke.

Downloaded From: https://complete.bioone.org/journals/Air,-Soil-and-Water-Research on 28 Mar 2024
Terms of Use: https://complete.bioone.org/terms-of-use

show moderate dynamic nature. In the middle part of the piedmont zone, the high dynamic natures of channel bars' width are noticed. It is strongly depicting that 63.15% of channel bar show very high dynamicity in past 20 years (Table 3). The similar dynamic character also observed in the lower part of this piedmont zone. Thus, 66.68% of channel bars' longest width show very dynamic behaviour since the 2000s.

Stability analysis of mid-channel bars

Development of channel bar is a continuous process in the Darjeeling Himalayan piedmont area. Riverbed deposition character depends on the seasonal deposition of sediment.[10] Flash flood is the usual phenomena of fluvial flood hydrology of North Bengal. Many of Eastern Himalayan foothill rivers such as Lish, Gish, Lethi, Murti, Kurti, Lethi, Jaldhaka, Teesta, Torsa, and Gish are affected by this type of phenomena. Seasonal flash floods, the huge amount of discharge (monsoon), the variation of incoming sediment have a formidable impact over the channel bars' growth. In the middle zone of piedmont area, the nature of area migration for 15.79% is very high (>1 km^2), 5.26% has high (0.75^{-1} km^2), 21.05% has moderate (0.50–0.75 km^2), 42.11% has low (0.25–0.50 km^2), and 15.79% has very low (<0.25 km^2). In the lower zone, 47.62% of area is under very high dynamicity, 14.29% is of moderate, 28.57% is of low, and 9.52% is of very low in nature (Table 4). Some of the bars are seasonally destroyed, some get migrated, and some new ones need to be accommodated. Channel bars 5, 9, 11, 13, 14, 16, 17, 33, 38, 43, 45, and 46 continuously show their dynamic nature which is basically under the lower and middle area of piedmont region (Figure 7). It is seen that in the upper zone of the piedmont area, since the 2000s, 58% to 72% channel bar area are stable. But in the middle and lower zones of the piedmont region, 26% to 42% and 14% to 29% area of the total channel bars is stable respectively (Figure 8).

Discussion

The considered area is a prominent state of the alluvial channel having a distinct aggradation process resulting in the formation of channel bar. Concerning the above-described methodology and after results analysis, it has been found that alteration of channel bar formation is a result of changing behaviour of the geo-hydrological processes and the effect of human interaction such as the construction of bridges, roads across the channel. Following the model of MCA PCA1, PCA2, and PCA3 for the rivers Teesta, Lish, Gish, Chel, Mal, Neora, Kurti, and Murti is scored as 86.67%, 53.33%, and 66.67%, respectively. Some observations have also been noticed in case of rivers Jaldhaka, Daina, and Torsa where the values of PCA1, PCA2, and PCA3 are 93.33%, PCA2 is 53.33% and PCA3 is 53.33%. The major concerned hydraulic components are water velocity, mean width, mean depth, wetted perimeter, hydraulic radius, cross-sectional area, water discharge, stream power, bed slope, inertial force, water depth (active), shear stress, and specific stream power. All these variables have been irregular from season to season. The comparison of erosion and deposition in respect of roughness also shows a distinct difference between upper and lower zones which depicts that within 1 year, bed roughness has been modified in the lower zone. The spatial pattern of stream power helps to make a clear concept of monsoon character. The huge variations of water discharge with enormous energy are resulting in huge sediment deposition along the channel.

Two empirical methods have been applied for the analysis of aggradations along the channel. Mobile depositions are analysed by empirical values of Foley[58] and Richardson.[59] The rivers Jaldhaka at Nagrakata, Teesta at Sevoke, and Torsa at Hasimara show high Foley values such as 2234.698, 1083.04, and 1102.613 kg $m^2 s^{-3}$, respectively, that are indicative of maximum erosion, thereby the lower parts of these points are zones of aggradations. The result of this empirical equation was validated with field observation which also showed similar results. Chel, Lish, and Gish are riverbed-aggraded rivers in North Bengal. The lowest values have provided directly comfortable sediment deposition zone. Bridge scouring is another factor for deposition in the lower part. The scouring values are maximum for Jaldhaka, Teesta, Torsa, and Chel rivers (0.64, 1.05, 0.55, and 0.73 m) at respective points as observed since 2016. Scouring depth and empirical values have negative relation where lower empirical values provide high erosion. The similar results were also observed from the table given above. Thus, from these observations, it is clear that the lower part of the bridge is the zone of high aggradation for bar formation.

The morphological study of the riverbed may speak about the general physical display of relief and slope bed and shows the prominent spatial variation of channel bars along the riverbed. The focused area has a huge vertical drop within short horizontal distance, from the downstream of the bridge where the reshaping of the bars is a continuous process. There is a prominent difference in height of bars between the upper and lower zones. The vertical height of upper, middle, and lower zones of respective channel bars are 5.1 to 0.2 m, 5.2 to 0.1 m, and 2.2 to 0.1 m. But the mean vertical elevations are 2.4, 1.8, and 0.9 m. The channel bar of the upper zone is stable concerning middle lower zone. Seasonal flash flood of the middle and lower zones of bars has changed the stability of bar nature. The bed elevation shows increase in Chel, Lish, and Gish which is the controlling factor of flow avulsion. Comparing the lower part of the bridge, if we analyse the cross section, there is a remarkable bifurcation of channels including active channels, seasonally active channels, and so on. Maximum flow avulsion is observed in the lower and middle zones of the piedmont area.

Size and longest length of the channel bars are very dynamic; in the upper zone, many of bars are stable since the 2000s because avulsion rate is low with respect to other

Downloaded From: https://complete.bioone.org/journals/Air,-Soil-and-Water-Research on 28 Mar 2024
Terms of Use: https://complete.bioone.org/terms-of-use

Downloaded From: https://complete.bioone.org/journals/Air,-Soil-and-Water-Research on 28 Mar 2024
Terms of Use: https://complete.bioone.org/terms-of-use

Table 3. Dynamic behaviour of decadal change of channel bars' longest width in the upper, middle, and lower part of piedmont zone.

NAME OF THE CHANNEL BARS	RIVERS	X	Y	$\Delta_{LW(i)}$	$\Delta_{LW(ii)}$	$\Delta_{LW(iii)}$	$\Delta_{LW(iv)}$	$\sum\Delta_{LW}$	REMARKS
Upper zone (>150 m)									
Bar 1	Teesta	26°52′12.39″N-26°52′46.45″N	88°28′30.40″E-88°28′31.84″E	0.26	0.08	−0.32	0.08	0.10	Very Low
Bar 2	Teesta	26°51′12.09″N-26°52′6.07″N	88°28′28.75″E-88°28′30.01″E	0.10	0.06	0.04	0.12	0.32	Low
Bar 3	Teesta	26°50′50.95″N-26°51′34.04″N	88°28′51.52″E-88°28′56.18″E	0.14	−0.42	0.02	0.70	0.44	Low
Bar 20	Gish	26°51′9.15″N-26°52′0.42″N	88°36′19.39″E-88°36′15.08″E	−0.14	0.34	0.04	0.02	0.26	Low
Bar 22	Chel	26°52′4.77″N-26°53′34.18″N	88°38′48.29″E-88°38′12.40″E	−0.08	0.02	0.06	0.01	0.01	Very Low
Bar 24	Mal	26°52′44.46″N-26°52′53.71″N	88°45′1.53″E-88°45′0.18″E	—	0.18	0.06	0.02	0.26	Low
Bar 26	Murti	26°51′46.29″N-26°52′22.46″N	88°49′58.79″E-88°49′58.83″E	0.10	0.54	−0.34	0.26	0.56	Moderate
Bar 27	Jaldhaka	26°52′25.10″N-26°53′49.82″N	88°53′41.26″E-88°53′44.79″E	0.46	0.40	0.04	−0.30	0.60	Moderate
Bar 28	Jaldhaka	26°52′17.09″N-26°52′27.02″N	88°53′40.10″E-88°53′38.61″E	0.16	0.06	0.04	0.02	0.28	Low
Bar 29	Jaldhaka	26°49′33.14″N-26°51′56.64″N	88°53′21.03″E-88°52′54.85″E	0.52	0.16	0.06	0.14	0.88	High
Middle zone (100-150 m)									
Bar 4	Teesta	26°50′32.84″N-26°51′26.42″N	88°29′0.52″E-88°29′26.90″E	0.08	−0.28	0.84	−0.14	0.50	Moderate
Bar 5	Teesta	26°45′38.34″N-26°48′58.07″N	88°31′46.34″E-88°34′16.35″E	0.82	−1.72	3.56	0.82	3.48	Very High
Bar 6	Teesta	26°45′49.86″N-26°47′22.92″N	88°33′3.57″E-88°34′16.38″E	1.22	1.56	−0.20	−0.08	2.5	Very High
Bar 7	Teesta	26°42′8.90″N-26°42′49.60″N	88°37′50.68″E-88°38′30.01″E	—	—	—	1.24	1.24	Very High
Bar 8	Teesta	26°41′36.46″N-26°42′35.79″N	88°36′53.35″E-88°37′20.85″E	—	—	—	1.32	1.32	Very High
Bar 9	Teesta	26°40′6.12″N-26°41′49.16″N	88°37′33.42″E-88°38′31.51″E	—	1.36	0.82	1.04	3.22	Very High
Bar 18	Lish	26°49′18.69″N-26°50′4.73″N	88°33′8.88″E-88°32′37.62″E	0.24	0.28	0.02	0.05	0.59	Moderate
Bar 19	Gish	26°47′29.43″N-26°48′25.24″N	88°35′17.74″E-88°34′56.37″E	0.94	−0.06	0.18	—	1.06	Very High
Bar 21	Chel	26°49′38.49″N-26°50′53.87″N	88°38′11.61″E-88°38′44.11″E	0.28	0.08	0.34	0.06	0.76	High
Bar 23	Chel	26°44′31.59″N-26°45′22.54″N	88°43′2.10″E-88°43′42.30″E	0.72	−0.06	0.22	−0.26	0.62	Moderate
Bar 25	Kumlai	26°47′15.38″N-26°47′56.59″N	88°45′29.48″E-88°45′27.22″E	0.04	0.26	−0.20	0.28	0.38	Low
Bar 30	Jaldhaka	26°50′1.99″N-26°51′6.67″N	88°53′17.32″E-88°53′5.34″E	0.4	0.46	0.06	0.08	1.00	Very High
Bar 31	Jaldhaka	26°48′43.55″N-26°50′24.54″N	88°53′28.81″E-88°53′22.82″E	0.16	−0.06	−0.26	0.04	0.12	Very Low
Bar 32	Jaldhaka	26°46′41.78″N-26°49′7.30″N	88°53′3.80″E-88°52′10.26″E	0.66	0.34	0.06	0.6	1.66	Very High
Bar 40	Rehti	26°44′3.07″N-26°44′50.57″N	89°5′47.77″E-89°5′52.62″E	—	0.98	0.41	0.03	1.42	Very High

(Continued)

Table 3. (Continued)

NAME OF THE CHANNEL BARS	RIVERS	X	Y	$\Delta_{LW(i)}$	$\Delta_{LW(ii)}$	$\Delta_{LW(iii)}$	$\Delta_{LW(iv)}$	$\sum\Delta_{LW}$	REMARKS
Bar 41	Torsa	26°45′15.53″N-26°46′18.81″N	89°19′48.02″E-89°19′34.73″E	0.3	−0.24	0.7	−1.00	0.24	Very Low
Bar 42	Torsa	26°44′11.59″N-26°45′5.49″N	89°19′33.01″E-89°19′26.52″E	1.6	−2.28	1.1	−0.62	0.2	Very Low
Bar 43	Torsa	26°44′56.70″N-26°47′38.17″N	89°19′38.20″E-89°19′9.30″E	0.42	1.46	0.2	−0.36	1.72	Very High
Bar 44	Torsa	26°42′28.72″N-26°43′6.17″N	89°19′38.58″E-89°19′48.68″E	0.82	0.28	0.58	−0.20	0.92	High
Lower zone (<100 m)									
10	Teesta	26°38′50.52″N-26°39′47.97″N	88°39′21.38″E-88°40′28.16″E	0.5	0.66	−2.21	0.81	0.24	Very Low
11	Teesta	26°36′8.02″N-26°39′17.49″N	88°38′58.50″E-88°42′37.43″E	2.34	1.43	0.17	1.39	5.33	Very High
12	Teesta	26°37′52.22″N-26°38′41.02″N	88°40′44.12″E-88°42′43.09″E	−0.08	−0.22	0.52	−0.28	0.06	Very Low
13	Teesta	26°37′22.55″N-26°38′38.00″N	88°42′43.54″E-88°43′52.53″E	1.10	1.81	−1.08	−2.90	1.06	Very High
14	Teesta	26°34′38.15″N-26°37′11.51″N	88°42′27.07″E-88°44′46.55″E	0.16	−1.88	1.32	−0.18	0.58	Moderate
15	Teesta	26°30′56.23″N-26°32′56.35″N	88°44′51.46″E-88°44′25.20″E	−0.34	1.16	−0.22	0.48	1.08	Very High
16	Teesta	26°29′45.83″N-26°31′31.15″N	88°45′19.22″E-88°44′28.10″E	−1.56	0.56	−1.46	0.8	1.66	Very High
17	Teesta	26°34′48.77″N-26°35′38.99″N	88°44′33.72″E-88°45′6.65″E	2.24	0.16	−2.00	2.24	2.64	Very High
33	Jaldhaka	26°39′16.23″N-26°42′7.82″N	88°52′9.87″E-88°51′57.33″E	0.26	0.38	−0.32	1.82	2.14	Very High
34	Jaldhaka	26°38′24.93″N-26°40′11.22″N	88°52′29.92″E-88°52′15.04″E	−0.26	0.32	−0.76	0.4	0.30	Low
35	Jaldhaka	26°36′55.97″N-26°38′49.75″N	88°52′39.08″E-88°53′18.98″E	0.07	0.98	0.1	−0.02	1.13	Very High
36	Jaldhaka	26°35′22.54″N-26°36′31.70″N	88°53′41.19″E-88°55′36.35″E	−0.40	0.56	0.76	0.08	1.00	Very High
37	Jaldhaka	26°30′57.19″N-26°32′3.22″N	88°58′45.73″E-89°1′49.92″E	−0.02	0.88	0.14	0.42	1.42	Very High
38	Jaldhaka	26°30′11.37″N-26°31′6.29″N	89°1′59.05″E-89°5′14.88″E	0.42	1.56	−0.70	2.56	3.84	Very High
39	Jaldhaka	26°29′48.27″N-26°30′26.62″N	89°2′50.76″E-89°5′19.86″E	0.4	−0.34	0.5	0.9	1.46	Very High
45	Torsa	26°40′1.37″N-26°41′3.30″N	89°19′25.04″E-89°19′52.04″E	0.7	0.1	1.26	0.96	1.1	Very High
46	Torsa	26°37′20.11″N-26°39′58.63″N	89°19′30.67″E-89°20′14.70″E	0.34	2.71	0.09	0.2	2.94	Very High
47	Torsa	26°36′54.92″N-26°37′37.91″N	89°20′36.35″E-26°36′54.92″N	0.02	−0.10	0.12	0.3	0.34	Low
48	Torsa	26°33′30.18″N-26°34′41.05″N	89°20′57.37″E-89°21′8.57″E	0.08	0.36	0.9	−0.16	1.18	Very High
49	Torsa	26°31′21.96″N-26°32′26.30″N	89°20′27.29″E-89°20′14.89″E	0.68	0.24	0.76	0.16	1.84	Very High
50	Torsa	26°29′38.74″N-26°30′16.95″N	89°19′35.00″E-89°19′10.95″E	0.52	0.4	−0.3	0.3	0.92	High

Downloaded From: https://complete.bioone.org/journals/Air,-Soil-and-Water-Research on 28 Mar 2024
Terms of Use: https://complete.bioone.org/terms-of-use

Downloaded From: https://complete.bioone.org/journals/Air,-Soil-and-Water-Research on 28 Mar 2024
Terms of Use: https://complete.bioone.org/terms-of-use

Table 4. Dynamic behaviour of decadal change of channel bar area in the upper, middle, and lower part of piedmont zone.

NAME OF THE CHANNEL BARS	RIVERS	X	Y	$\Delta_{A(i)}$ km²	$\Delta_{A(ii)}$ km²	$\Delta_{A(iii)}$ km²	$\Delta_{A(iv)}$ km²	$\sum\Delta_A$ km²	DYNAMIC BEHAVIOUR
Upper zone (>150 m)									
Bar 1	Teesta	26°52′12.39″N-26°52′46.45″N	88°28′30.40″E-88°28′31.84″E	0.0908	−0.1554	−0.0958	0.031	0.1294	Very low
Bar 2	Teesta	26°51′12.09″N-26°52′6.07″N	88°28′28.75″E-88°28′30.01″E	0.2352	−0.1008	0.1940	0.0388	0.3672	Low
Bar 3	Teesta	26°50′50.95″N-26°51′34.04″N	88°28′51.52″E-88°28′56.18″E	0.2568	−0.2600	0.1068	0.2856	0.3892	Low
Bar 20	Gish	26°51′9.15″N-26°52′0.42″N	88°36′19.39″E-88°36′15.08″E	−0.0836	0.4700	0.1752	0.0116	0.5732	Moderate
Bar 22	Chel	26°52′4.77″N-26°53′34.18″N	88°38′48.29″E-88°38′12.40″E	0.3728	0.7796	0.1576	−0.7336	0.5764	Moderate
Bar 24	Mal	26°52′44.46″N-26°52′53.71″N	88°45′1.53″E-88°45′0.18″E	—	0.2160	−0.1872	0.0024	0.0312	Very low
Bar 26	Murti	26°51′46.29″N-26°52′22.46″N	88°49′58.79″E-88°49′58.83″E	0.0336	0.0624	−0.0612	0.026	0.0608	Very low
Bar 27	Jaldhaka	26°52′25.10″N-26°53′49.82″N	88°53′41.26″E-88°53′44.79″E	0.0828	0.0156	0.0636	0.0484	0.2104	Very low
Bar 28	Jaldhaka	26°52′17.09″N-26°52′27.02″N	88°53′40.10″E-88°53′38.61″E	0.0216	0.0048	0.0048	0.0024	0.0336	Very low
Bar 29	Jaldhaka	26°49′33.14″N-26°51′56.64″N	88°53′21.03″E-88°52′54.85″E	0.1144	0.4472	0.0192	0.1312	0.712	Moderate
Middle zone (100-150 m)									
Bar 4	Teesta	26°50′32.84″N-26°51′26.42″N	88°29′0.52″E-88°29′26.90″E	−0.124	0.0492	0.620	−0.4088	0.1364	Very low
Bar 5	Teesta	26°45′38.34″N-26°48′58.07″N	88°31′46.34″E-88°34′16.35″E	0.208	−0.4104	2.114	0.2112	2.1237	High
Bar 6	Teesta	26°45′49.86″N-26°47′22.92″N	88°33′3.57″E-88°34′16.38″E	0.651	1.3816	2.11	0.3444	0.2672	Low
Bar 7	Teesta	26°42′8.90″N-26°42′49.60″N	88°37′50.68″E-88°38′30.01″E	—	—	—	0.4536	0.4536	Low
Bar 8	Teesta	26°41′36.46″N-26°42′35.79″N	88°36′53.35″E-88°37′20.85″E	—	—	—	0.3421	0.3421	Low
Bar 9	Teesta	26°40′6.12″N-26°41′49.16″N	88°37′33.42″E-88°38′31.51″E	—	0.6528	0.8296	0.8360	2.3184	Very High
Bar 18	Lish	26°49′18.69″N-26°50′4.73″N	88°33′8.88″E-88°32′37.62″E	0.056	0.5576	0.044	0.0646	0.7222	Moderate
Bar 19	Gish	26°47′29.43″N-26°48′25.24″N	88°35′17.74″E-88°34′56.37″E	0.2944	0.282	0.3772	−0.2576	0.6960	Moderate
Bar 21	Chel	26°49′38.49″N-26°50′53.87″N	88°38′11.61″E-88°38′44.11″E	0.256	−0.184	0.518	0.1356	0.7256	Moderate
Bar 23	Chel	26°44′31.59″N-26°45′22.54″N	88°43′2.10″E-88°43′42.30″E	0.3364	−0.1912	0.1648	−0.0056	0.3044	Low
Bar 25	Kumlai	26°47′15.38″N-26°47′56.59″N	88°45′29.48″E-88°45′27.22″E	0.0864	0.0096	0.034	−0.0084	0.1216	Very Low
Bar 30	Jaldhaka	26°50′1.99″N-26°51′6.67″N	88°53′17.32″E-88°53′5.34″E	0.1128	0.4588	−0.0936	0.0660	0.5440	Moderate
Bar 31	Jaldhaka	26°48′43.55″N-26°50′24.54″N	88°53′28.81″E-88°53′22.82″E	−0.8888	0.3048	0.0648	0.0424	0.4768	Low
Bar 32	Jaldhaka	26°46′41.78″N-26°49′7.30″N	88°53′3.80″E-88°52′10.26″E	0.6252	0.1768	0.0312	0.0432	0.8764	Moderate
Bar 40	Rehti	26°44′3.07″N-26°44′50.57″N	89°5′47.77″E-89°5′52.62″E	—	0.2016	0.1598	0.0078	0.3692	Low
Bar 41	Torsa	26°45′15.53″N-26°46′18.81″N	89°19′48.02″E-89°19′34.73″E	0.2476	−0.006	0.5184	−0.7392	0.0208	Very low

(Continued)

Table 4. (Continued)

NAME OF THE CHANNEL BARS	RIVERS	X	Y	$\Delta_{A(i)}$ km^2	$\Delta_{A(ii)}$ km^2	$\Delta_{A(iii)}$ km^2	$\Delta_{A(iv)}$ km^2	$\sum\Delta_A$ km^2	DYNAMIC BEHAVIOUR
Bar 42	Torsa	26°44′11.59″N-26°45′5.49″N	89°19′33.01″E-89°19′26.52″E	−0.2656	−0.7288	0.8132	−0.2372	0.4184	Low
Bar 43	Torsa	26°44′56.70″N-26°47′38.17″N	89°19′38.20″E-89°19′9.30″E	1.3100	2.094	0.193	−0.7650	2.8320	Very High
Bar 44	Torsa	26°42′28.72″N-26°43′6.17″N	89°19′38.58″E-89°19′48.68″E	0.2788	0.16	0.1298	0.0090	0.2576	Low
Lower zone (<100 m)									
10	Teesta	26°38′50.52″N-26°39′47.97″N	88°39′21.38″E-88°40′28.16″E	1.724	1.006	−3.8908	0.5584	0.6016	Moderate
11	Teesta	26°36′8.02″N-26°39′17.49″N	88°38′58.50″E-88°42′37.43″E	2.848	3.430	1.6704	−2.0184	5.9316	Very High
12	Teesta	26°37′52.22″N-26°38′41.02″N	88°40′44.12″E-88°42′43.09″E	−0.270	−0.242	1.4396	−1.2376	0.3104	Low
13	Teesta	26°37′22.55″N-26°38′38.00″N	88°42′43.54″E-88°43′52.53″E	1.5764	−1.730	1.4844	−2.4492	1.1188	Very High
14	Teesta	26°34′38.15″N-26°37′11.51″N	88°42′27.07″E-88°44′46.55″E	2.2104	−3.092	2.9304	−0.6336	1.4144	Very High
15	Teesta	26°30′56.23″N-26°32′56.35″N	88°44′51.46″E-88°44′25.20″E	−0.996	1.684	−1.3224	0.7400	0.1064	Very Low
16	Teesta	26°29′45.83″N-26°31′31.15″N	88°45′19.22″E-88°44′28.10″E	−3.138	0.938	−1.7860	1.8308	2.1544	Very High
17	Teesta	26°34′48.77″N-26°35′38.99″N	88°44′33.72″E-88°45′6.65″E	2.18	−0.288	0.9640	2.5704	5.436	Very High
33	Jaldhaka	26°39′16.23″N-26°42′7.82″N	88°52′9.87″E-88°51′57.33″E	0.765	1.187	−1.1500	2.1604	2.9628	Very High
34	Jaldhaka	26°38′24.93″N-26°40′11.22″N	88°52′29.92″E-88°52′15.04″E	−0.077	0.248	−0.8760	0.6672	0.0372	Very Low
35	Jaldhaka	26°36′55.97″N-26°38′49.75″N	88°52′39.08″E-88°53′18.98″E	−0.08	1.982	0.4580	0.7296	3.0926	Very High
36	Jaldhaka	26°35′22.54″N-26°36′31.70″N	88°53′41.19″E-88°55′36.35″E	−0.441	0.547	0.3600	0.1944	0.6600	Moderate
37	Jaldhaka	26°30′57.19″N-26°32′3.22″N	88°58′45.73″E-89°1′49.92″E	0.298	−0.522	0.4892	0.2032	0.468	Low
38	Jaldhaka	26°30′11.37″N-26°31′6.29″N	89°1′59.05″E-89°5′14.88″E	0.902	0.917	−0.4456	2.3328	3.7064	Very High
39	Jaldhaka	26°29′48.27″N-26°30′26.62″N	89°2′50.76″E-89°5′19.86″E	−0.292	−0.116	0.7656	−0.7848	0.4272	Low
45	Torsa	26°40′1.37″N-26°41′3.30″N	89°19′25.04″E-89°19′52.04″E	0.693	0.090	0.9332	−0.4132	1.1232	Very High
46	Torsa	26°37′20.11″N-26°39′58.63″N	89°19′30.67″E-89°20′14.70″E	0.665	2.825	−0.9502	1.3520	3.8928	Very High
47	Torsa	26°36′54.92″N-26°37′37.91″N	89°20′36.35″E-26°36′54.92″N	−0.010	0.030	0.0400	0.2876	0.3484	Low
48	Torsa	26°33′30.18″N-26°34′41.05″N	89°20′57.37″E-89°21′8.57″E	−0.008	0.272	0.3420	0.0148	0.6208	Moderate
49	Torsa	26°31′21.96″N-26°32′26.30″N	89°20′27.29″E-89°20′14.89″E	0.122	0.172	0.3440	−0.2336	0.4048	Low
50	Torsa	26°29′38.74″N-26°30′16.95″N	89°19′35.00″E-89°19′10.95″E	0.037	0.128	−0.0664	0.2504	0.3496	Low

Downloaded From: https://complete.bioone.org/journals/Air,-Soil-and-Water-Research on 28 Mar 2024
Terms of Use: https://complete.bioone.org/terms-of-use

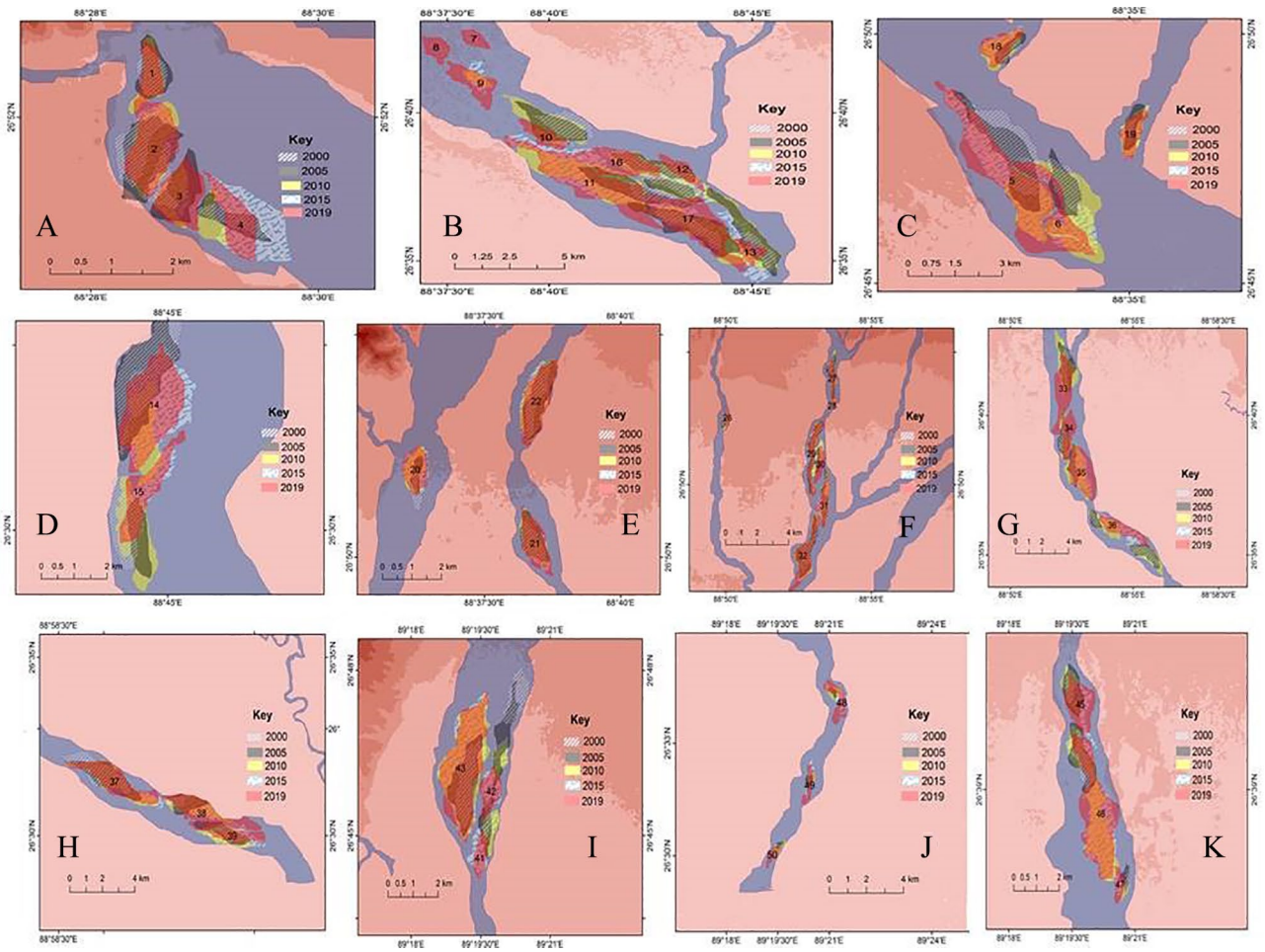


Figure 7. Migration of channel bars since 2000 in Darjeeling Himalayan foothills zone: (A) Teesta River near Sevoke, (B) Teesta River near Kranti, (C) Teesta River near Hanskhali, (D) Teesta River near Maynaguri, (E) Chel River near Odlabari, (F) Jaldhaka River near Nagrakata, (G) Jaldhaka River near Panbari, (H) Jaldhaka River near Dhupguri-Falakata, (I) Torsa River near Hasimara, (J) Torsa River near Mathurabagan, and (K) Torsa River near Madarihat.

positions. Change of bars area and its longest width have positive relation ($R^2 = .627$) (Figure 9). Here, in the upper zone stream power, velocity and discharge are high but the rate of deposition is very low. The nature of dynamicity in the area of the channel bars in the upper zone is 0.12 to 0.71 km^2 which is very low but the bars 20, 22, and 29 show moderate dynamic nature. In the middle and lower zones of the piedmont area, channel bars have very high dynamicity in their size, shape, and length. In the middle and lower zones, the rate of alteration in area is 0.12 to 2.83 km^2 and 0.1 to 5.43 km^2 repectively (Figure 10). Huge changes of velocity, granulometric character of sediment, change of channel gradient, and upstream landslide are major considering factors for this dynamicity. Sometimes large bars are divided into some fragmented-part by the seasonal active channel and also a single bar may form by joining with many smallar one. So, the morphodynamic alteration is frequently observed in the lower-middle zone where the accommodation and destruction processes of channel bars are found.

Conclusions

This research reports on formation, migration, and morphodynamic alteration of 50 channel bars in Darjeeling Himalayan piedmont zone. The rivers in the foothills of Darjeeling Himalayas in the northern part of the state of West Bengal are flowing over a region of active tectonic activities. This has resulted in the formation of extraordinary features on the bed of the rivers and the development of meso and micro channel bars. The original outcome of the research is the result of several field verifications and primary to the secondary database. The quantitative data set provided major bars are dynamic nature in a life period due to their huge change of hydro-geomorphic behaviour. The change of fluvial hydraulics, spatial variation of aggradation, and degradation are responses over this dynamic nature. Spatially, the huge amount of seasonal cohesive sediment and variation in discharge bring changes in the channel bars' size, shape, and stability in response to the variation of altitude and gradient from the foothill to the lower reach of the channels. The

Downloaded From: https://complete.bioone.org/journals/Air,-Soil-and-Water-Research on 28 Mar 2024
Terms of Use: https://complete.bioone.org/terms-of-use

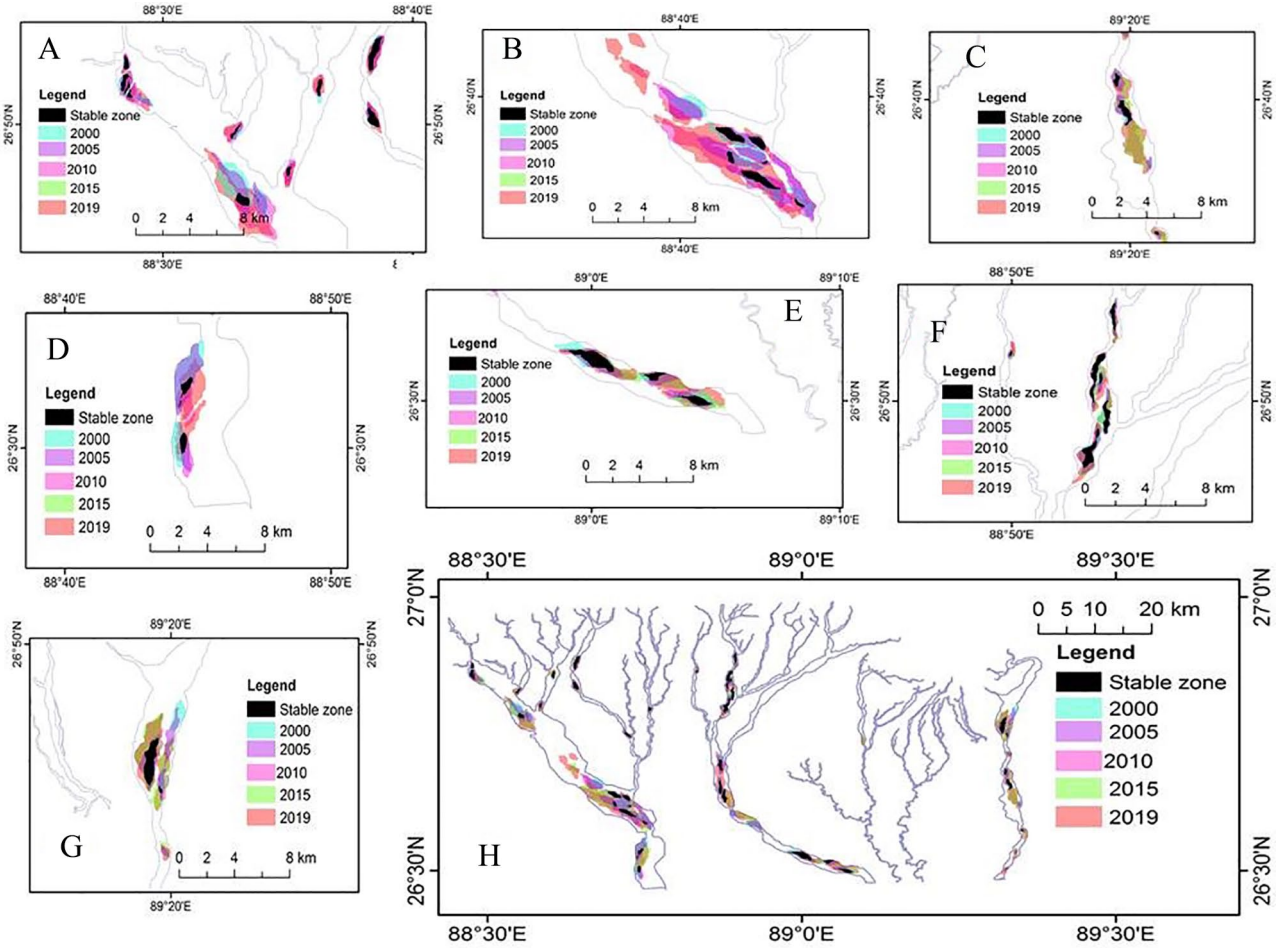


Figure 8. Site-wise channel bar stability in Darjeeling Himalayan foothill zone: (A) Teesta, Lish, Gish, and Chel River (Sevoke, Hanskhali, Odlabari); (B) Teesta River near Kranti; (C) Torsa River near Madarihat; (D) Teesta River near Maynaguri; (E) Jaldhaka River near Dhupguri-Falakata; (F) Jaldhaka near Nagrakata; (G) Torsa River near Hasimara; (H) Total study area of Darjeeling Himalayan foothill region.

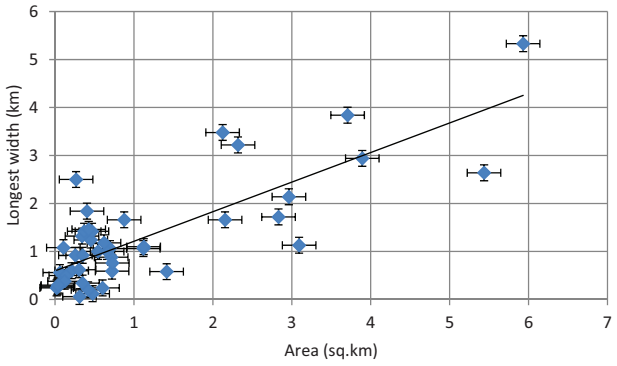


Figure 9. Correlation between channel bar area and longest width of selective 50 channel bars.

natural factors have initiated the formation but anthropogenic factors have aggravated the situation and sometimes even lead to a misbalance in the natural regime. The constructions of the bridges across the river have changed the configuration of channel bars due to their changing flow pattern. From the investigation, it has also been depicted that bridges have stronger influence on the morphology of the bars as compared with the sediment influx by monsoonal rainfall. Rate of degradation and aggradation of the channel has been exaggerated by the presence of bridges. This could be a major reason for the dynamic activity of the bars in the middle and lower zones where bridges are present. As per the environmental concentration, piedmont stable channel bars are useful for settlement habitations, seasonal agriculture, and social forestry. The gravel, sand, and heterogeneous sediment of unstable channel bars are also helpful for building construction purpose. The local government, authority of environmental management, and river institutions should pay prime attention on these considered piedmont channel bars for sustainable river management plan.

Acknowledgements

We convey our special thanks to USGS Earth Explorer, ArcGIS 10.2.2 software, IBM SPSS 22 software, and Google Earth application providing some data and supporting for creation of maps. We are also thankful to the Editor-in-Chief

Downloaded From: https://complete.bioone.org/journals/Air,-Soil-and-Water-Research on 28 Mar 2024
Terms of Use: https://complete.bioone.org/terms-of-use

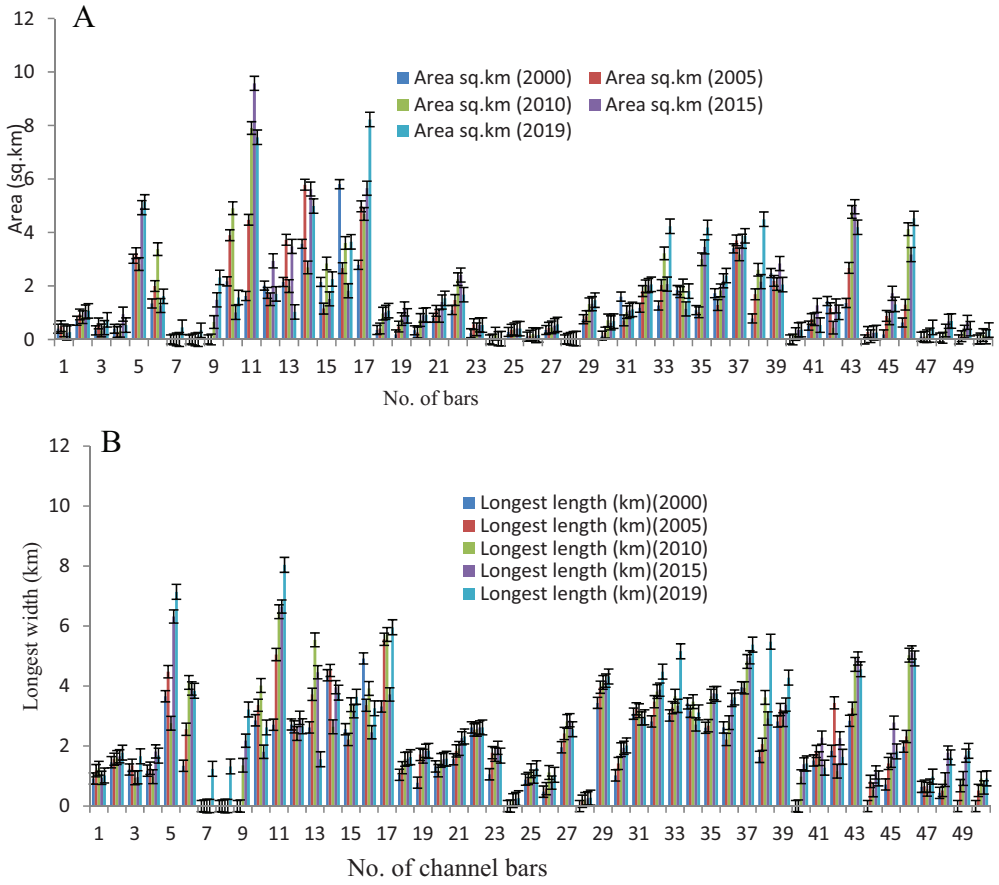


Figure 10. Channel bars' dynamicity of selective 50 bars: (A) size aspect and (B) longest width aspect in Darjeeling Himalayan piedmont zone.

Erick R. Bandala (Water section), Commissioning Editor Bree Sundling and the anonymous reviewers for their valuable comments to substantial improvement of the manuscript.

Author Contributions

First author as a research scholar has done this research work under the supervision of second author, all authors have made equal efforts for construction of this manuscript.

ORCID iD

Md Kutubuddin Dhali https://orcid.org/0000-0001-8112-2437

REFERENCES

1. Fujita Y. Bar and channel formation in braided streams. In: Ikeda S, Parker G, eds. *River Meandering, American Geophysical Union* (Water Resources Monographs, Vol. 12); 1989:417-462.
2. Jiongxin X. Evolution of mid-channel bars in a braided river and complex response to reservoir construction: an example from the middle Hanjiang River, China. *Earth Surf Process Landf*. 1997;22:953-965. doi:10.1002/(sici)1096-9837(199710)22:10<953::aid-esp789>3.0.co;2-s.
3. Surian N, Rinaldi M. Morphological response to river engineering and management in alluvial channels in Italy. *Geomorphology*. 2003;50:307-326.
4. Fan H, Huang H, Zeng TQ , Wang K. River mouth bar formation, riverbed aggradation and channel migration in the modern Huanghe (Yellow) River delta, China. *Geomorphology*. 2006;74:124-136.
5. Batalla R, Vericat D, Martínez T. River-channel changes downstream from dams in the lower Ebro River. *Z Geomorphol*. 2006;143(Suppl. B):1-14.
6. Belletti B, Dufour S, Piégay H. What is the relative effect of space and time to explain the Braided River width and island patterns at a regional scale? *River Res Appl*. 2015;31:1-15. doi:10.1002/rra.2714.
7. Petts GE, Gurnell AM. Dams and geomorphology: research progress and future directions. *Geomorphology*. 2005;71:27-47.
8. Crosato A, Mosselman E. Simple physics-based predictor for the number of river bars and the transition between meandering and braiding. *Water Resour Res*. 2009;45:W03424.
9. Alexander J, Cooker MJ. Moving boulders in flash floods and estimating flow conditions using boulders in ancient deposits. *Sedimentology*. 2016;63:1582-1595. doi:10.1111/sed.12274.
10. Dhali MK, Ayaz S, Sahana M, Guha S. Response of sediment flux, bridge scouring on river bed morphology and geomorphic resilience in middle-lower part of river Chel, Eastern Himalayan foothills zone, India. *Ecol Eng*. 2020;142:105632. doi:10.1016/j.ecoleng.2019.105632.
11. Surian N. Downstream variation in grain size along an Alpine river: analysis of controls and processes. *Geomorphology*. 2002;43:137-149.
12. Bandyopadhyay S, Kar NS, Das S, Sen J. River systems and water resources of West Bengal: a review. *Geol Soc Spec Publ*. 2014;3:63-84.
13. Vorosmarty CJ, Meybeck M, Fekete B, Sharma K, Green P, Syvitski JPM. Anthropogenic sediment retention: major global impact from registered river impoundments. *Glob Planet Chang*. 2003;39:169-190.
14. Walling DE, Fang D. Recent trends in the suspended sediment loads of the world's rivers. *Glob Planet Chang*. 2003;39:111-126.
15. Walling DE. Human impact on land-ocean sediment transfer by the world's rivers. *Geomorphology*. 2006;79:192-216.
16. Wang B, Xu YJ. Dynamics of 30 large channel bars in the Lower Mississippi River in response to river engineering from 1985 to 2015. *Geomorphology*. 2018;300:31-44.
17. Yang Z, Wang H, Saito Y, et al. Dam impacts on the Changjiang (Yangtze) River sediment discharge to the sea: the past 55 years and after the Three Gorges Dam. *Water Resour Res*. 2006;42:W04407.
18. Meade RH, Moody JA. Causes for the decline of suspended-sediment discharge in the Mississippi River system, 1940–2007. *Hydrol Process*. 2010;24:35-49.

Downloaded From: https://complete.bioone.org/journals/Air,-Soil-and-Water-Research on 28 Mar 2024
Terms of Use: https://complete.bioone.org/terms-of-use

19. Wang B, Xu YJ. Sediment trapping by emerged channel bars in the Lowermost Mississippi River during a major flood. *Water*. 2015;7:6079-6096.
20. Wang B, Xu YJ. Long-term geomorphic response to flow regulation in a 10-km reach downstream of the Mississippi–Atchafalaya River diversion. *J Hydrol Reg Stud*. 2016;8:10-25.
21. Dhali K, Sahana M. Spatial variation in fluvial hydraulics with major bed erosion zone: a study of Kharsoti river of India in the post monsoon period. *Arabian Journal of Geosciences*. 2017;10:451.
22. Sarkar S. Flood hazard in the sub-Himalayan North Bengal, India. In: Singh S, Starkel L, Syiemlieh HJ, eds. *Environmental Changes and Geomorphic Hazard*. New Delhi, India: Bookwell; 2008:247-262.
23. Ghosh D. Determining process of occasional flooding from channel hydrological characteristics of Chel Basin, North Bengal (India). *Spat Inf Res*. 2020;28:313-326. doi:10.1007/s41324-019-00290-0.
24. Lama S, Maiti R. Morphometric analysis of Chel River Basin, West Bengal, India, using geographic information system. *Earth Sci India*. 2019;12:1-23.
25. Yang SL, Milliman JD, Li P, Xu K. 50,000 dams later: erosion of the Yangtze River and its delta. *Glob Planet Chang*. 2011;75:14-20.
26. Blum MD, Roberts HH. Drowning of the Mississippi Delta due to insufficient sediment supply and global sea-level rise. *Nat Geosci*. 2009;2:488-491.
27. Sanyal J. Predicting possible effects of dams on downstream river bed changes of a Himalayan river with morphodynamic modelling. *Quater Int*. 2017;453:48-62. doi:10.1016/j.quaint.2017.03.063.
28. Hu BQ , Yang ZS, Wang HJ, Sun XX, Bi NS, Li GG. Sedimentation in the Three Gorges Dam and the future trend of Changjiang (Yangtze River) sediment flux to the sea. *Hydrol Earth Syst Sci*. 2009;13:2253-2264.
29. Qin YS, Li F. Study of the influence of sediment loads discharged from Huanghe River on sedimentation in the Bohai and Yellow seas. *Studia Marina Sinica*. 1986;27:125-135 (in Chinese with English abstract).
30. Van Gelder A, Van den Berg JH, Cheng G, Xue C. Overbank and channel fill deposits of the modern Yellow River delta. *Sedimen Geol*. 1994;90:293-305.
31. Xu J. River sedimentation and channel adjustment of the lower Yellow River as influenced by low discharges and seasonal channel dry-ups. *Geomorphology*. 2002;43:151-164.
32. Rodrigues S, Mosselman E, Claude N, Wintenberger CL, Juge P. Alternate bars in a sandy gravel bed river: generation, migration and interactions with superimposed dunes. *Earth Surf Process Planforms BGRG*. 2015;40:610-628. doi:10.1002/esp.3657.
33. Edmonds DA, Slingerland RL. Mechanics of river mouth bar formation: implications for the morphodynamics of delta distributary networks. *J Geophys Res*. 2007;112:F02034. doi:10.1029/2006JF000574.
34. Li Z, Wang Z, Pan B, Zhu H, Li W. The development mechanism of gravel bars in rivers. *Quater Int*. 2013;336:73-79. doi:10.1016/j.quaint.2013.12.039.
35. Shampa S, Ali M. Development of bars in a large sand bed braided rivers. Paper presented at: Small Scale Morphological Evolution of Coastal, Estuarine and River Systems (Société Hydrotechnique de France) (ed P-L Viollet); October 6-7, 2014; Nantes, France:3-7.
36. Shampa S, Ali M. Numerical modeling of bar dynamics of a sand-bed braided river. Paper presented at: 5th International Conference on Water and Flood Management; March 6-8, 2015; Dhaka, Bangladesh:41-52.
37. Shampa S, Ali M. Interaction between the braided bar and adjacent channel during flood: a case study of a sand-bed braided river, Brahmaputra–Jamuna. *Sustain Water Res Manage*. 2019;5:947-960. doi:10.1007/s40899-018-0269-x.
38. Zhang X, Li M, Li Y, Sun J. Experimental study on bar formation in a scouring process. *Nat Hazards*. 2017;89:723-740. doi:10.1007/s11069-017-2989-x.
39. Colombini M, Seminara G, Tubino M. Finite-amplitude alternate bars. *J Fluid Mech*. 1987;181:213-232. doi:10.1017/S0022112087002064.
40. Blondeaux P, Seminara G. A unified bar bend theory of river meanders. *J Fluid Mech*. 1985;157:449-470. doi:10.1017/S0022112085002440.
41. Tubino M, Seminara G. Free-forced interactions in developing meanders and suppression of free bars. *J Fluid Mech*. 1990;214:131-159. doi:10.1017/s0022112090000088.
42. Siviglia A, Stecca G, Vanzo D, Zolezzi G, Toro EF, Tubino M. Numerical modelling of two-dimensional morphodynamics with applications to river bars and bifurcations. *Adv Water Resour*. 2013;53:243-260. doi:10.1016/j.advwatres.2012.11.010.
43. Schuurman F, Marra WA, Kleinhans MG. Physics-based modeling of large braided sand-bed rivers: bar pattern formation, dynamics, and sensitivity. *J Geophys Res: Earth Surf*. 2013;118:2509-2527. doi:10.1002/2013jf002896.
44. Asworth PJ, Best JL, Roden JE, Bristow CS, Klaassen GJ. Morphological evolution and dynamics of a large, sand braid-bar, Jamuna River, Bangladesh. *Sedimentology*. 2000;47:533-555. doi:10.1046/j.1365-3091.2000.00305.x.
45. Smith DG, Hubbard SM, Leckie DA, Fustic M. Counter point bar deposits: lithofacies and reservoir significance in the meandering modern Peace River and ancient McMurray Formation, Alberta, Canada. *Sedimentology*. 2009;56:1655-1669. doi:10.1111/j.1365-3091.2009.01050.x.
46. Hooke JM. The significance of mid-channel bars in an active meandering river. *Sedimentology*. 1986;33:839-850.
47. Ayaz S, Biswas M, Dhali MK. Morphotectonic analysis of alluvial fan dynamics: a comparative study in spatio-temporal scale of Himalayan foothill, India. *Arab J Geosci*. 2018;11:Article 41. doi:10.1007/s12517-017-3308-2.
48. Ayaz S, Dhali MK. Longitudinal profiles and geomorphic indices analysis on tectonic evidence of fluvial form, process and landform deformation of Eastern Himalayan Rivers, India. *Geol Ecol Landsc*. 2019;4:11-22. doi:10.1080/24749508.2019.1568130
49. Acharya SK. A note on the nature of Daling-Darjeeling relation, Darjeeling hills. *Indus Min*. 1971;25:254-255.
50. Mukul M, Jade S, Ansari K, Matin A. Seismotectonic implications of strike-slip earthquakes in the Darjiling–Sikkim Himalaya. *Curr Sci*. 2014;106:198-210.
51. Mullick M, Riguzzi F, Mukhopadhyay D. Estimates of motion and strain rates across active faults in the frontal part of eastern Himalayas in North Bengal from GPS measurements. *Terra Nova*. 2009;21:410-415.
52. Nakata T. Active faults of the Himalaya of India and Nepal. *Geol Soc Am Spec Paper*. 1989;232:243-264.
53. Chakraborty T, Ghosh P. The geomorphology and sedimentology of the Tista-megafan, Darjeeling Himalaya: implications for megafan building processes. *Geomorphology*. 2010;115:252-266.
54. Walker W, Harremoës P, Rotmans J, Van der Sluijs J, Van Asselt MBA, Jansen P. Defining uncertainty: a conceptual basis for uncertainty management in model-based decision support. *J Integr Assess*. 2003;4:5-17.
55. Konidari P, Mavrakis D. A multi-criteria evaluation method for climate change mitigation policy instruments. *Energ Pol*. 2007;35:6235-6257.
56. Dhali MK, Biswas M. MCA on mechanism of river bed potholes growth: a study of middle Subarnarekha River Basin, South East Asia. *Environ Develop Sustain*. 2019;21:935-959. doi:10.1007/s10668-017-0069-8.
57. Charlton RO. *Fundamentals of Fluvial Geomorphology*. Abingdon, UK: Routledge; 2007:10-107.
58. Foley MG. Bed-rock incision by streams. *Geol Soc Am Bull Part II*. 1980;91:2189-2213.
59. Richardson EV, Simons DB, Karaki S, Mahmood K, Stevens MA. *Highways in the River Environment*. 1st ed. Fort Collins, CO: FHWA, U.S. Department of Transportation; 1975.
60. Prokop P, Sarkar S. Natural and human impact on land use change of the Sikkimese-Bhutanese Himalayan piedmont, India. *Quaestionesgeogr*. 2012;31:63-75. doi:10.2478/v10117-012-0010-z.
61. Wiejaczka L. Riverbeds level changes in the margin and foreland of the Darjeeling Himalaya during the years with a normal monsoon, rainfall. In: Singh RB, Prokop P, eds. *Environmental Geography of South Asia, Advances in Geographical and Environmental Sciences*; 2016. doi:10.1007/978-4-431-55741-8_5.
62. Pate P. GIS techniques for landscape analysis – case study of the Chel River Basin. Paper presented at: State Level Seminar on Geographical Methods in the Appraisal of Landscape; March 20, 2012; Kolkata, India:1-14.
63. Dhali MK. Dynamic evolution of riverbed potholes in the granitic bedrock of Chota Nagpur Plateau, Middle part of Subarnarekha River basin, India. *J Hydrol*. 2019;571:819-836. doi:10.1016/j.jhydrol.2019.02.022.

Downloaded From: https://complete.bioone.org/journals/Air,-Soil-and-Water-Research on 28 Mar 2024
Terms of Use: https://complete.bioone.org/terms-of-use